Editors' Suggestion

Background-Free Measurement of Ring Currents by Symmetry-Breaking High-Harmonic Spectroscopy

Ofer Neufeld* and Oren Cohen†
Physics Department and Solid State Institute, Technion—Israel Institute of Technology, Haifa 32000, Israel

(Received 13 May 2019; published 6 September 2019)

We propose and explore an all-optical technique for ultrafast characterization of electronic ring currents in atoms and molecules, based on high-harmonic generation (HHG). In our approach, a medium is irradiated by an intense reflection-symmetric laser pulse that leads to HHG, where the polarization of the emitted harmonics is strictly linear if the medium is reflection invariant (e.g., randomly oriented atomic or molecular media). The presence of a ring current in the medium breaks this symmetry, causing the emission of elliptically polarized harmonics, where the harmonics' polarization directly maps the ring current, and the signal is background-free. Scanning the delay between the current excitation and the HHG driving pulse provides an attosecond time-resolved signal for the multielectron dynamics in the excited current (including electron-electron interactions). We analyze the responsible physical mechanism and derive the analytic dependence of the HHG emission on the ring current. The method is numerically demonstrated using quantum models for neon and benzene, as well as through *ab initio* calculations.

DOI: 10.1103/PhysRevLett.123.103202

Excited atoms and molecules can carry electric currents that circulate in microscopic media. From a quantum mechanical perspective, these currents are understood as a coherent wave packet comprising a superposition of bound states, causing the wave function to oscillate in time [1–6]. If this wave packet carries angular momentum, ring currents circulate in the medium. For instance, a hydrogen atom excited to a $2p$ state with nonzero magnetic quantum number m carries a ring current. More complex systems can also carry ring currents, e.g., spin-orbit wave packets in atoms [7] or multielectron wave packets in larger molecules, such as Mg-porphyrin [3]. This phenomenon is general to any high-dimensional ($d > 1$) quantum system and is especially interesting because it typically occurs on the natural timescale of electronic motion—attoseconds to femtoseconds. Understanding ring currents can thus pave the way for manipulating and controlling ultrafast processes on the nanoscale, including chemical bond formation and topologically protected currents [8,9], as well as for the generation of intense magnetic field pulses [10,11]. However, electronic ring currents within atoms and molecules are very difficult to detect and, consequently, also very difficult to control.

Traditional approaches to generate and analyze ring currents rely on the application of strong magnetic fields [12], sacrificing the temporal resolution. More recent proposals suggest optically exciting a current (either by an optical resonant excitation [3,4] or by ionization [13–16]) and subsequently probing it with a second ionizing pulse [17–19]. This method was recently experimentally demonstrated in argon [6] and requires angularly, temporally, and energetically resolving photoelectrons.

An alternative promising idea is to probe ring currents using high-harmonic spectroscopy, which is a powerful all-optical tabletop technique that, for example, was successfully used to detect ultrafast charge migration [20]. So far, the only work in this direction theoretically investigated high-harmonic generation (HHG) driven by few cycle monochromatic elliptical pulses in a medium with a strong single electron ring current state [13]. They showed that the HHG yield uniquely depends on the pump's ellipticity, particularly in the cutoff region; however, the dependence on the current density was not explored. Moreover, using this scheme for exploring ultrafast ring currents would be very challenging because (i) the differential HHG response using this approach is relatively weak, (ii) it does not exhibit one-to-one correspondence to the current density, and (iii) the elliptical pulse itself generates a current in the medium, which disrupts the measurement process and its temporal resolution.

Here, we propose and theoretically explore a novel approach for ultrafast ring current characterization in media that at zero current exhibits reflection symmetry (e.g., isotropic gas or liquid, aligned molecular gas with a reflection symmetry, and reflection-invariant crystals). The scheme relies on fundamental symmetry considerations in HHG, where the driving pulse is specifically chosen to exhibit a reflection symmetry that standardly leads to linearly polarized harmonic selection rules [21]. However, if the medium carries ring currents, this symmetry-based selection rule is broken, causing the emission of elliptically polarized harmonics. The emitted harmonic ellipticities exhibit direct one-to-one scaling to the ring current, which we analytically derive, providing a robust

background-free signal. This scheme can be implemented using linearly polarized monochromatic pumps and colinearly or cross-linearly polarized bichromatic pumps, making it highly versatile. We numerically demonstrate the technique using quantum models for neon and benzene systems, and *ab initio* time-dependent density functional theory (TDDFT) calculations. Lastly, our *ab initio* calculations reveal that electron-electron (*e*-*e*) interactions induce attosecond multielectron dynamics in the current-carrying states, which are mapped onto the high-harmonic response and are detectable within our scheme.

We first outline our approach. The Hamiltonian of the HHG process is given by

$$\mathscr{H} = \mathscr{H}_0 + \mathscr{H}_{\mathrm{int}}(t), \tag{1}$$

where $\mathscr{H}_0$ is a field-free Hamiltonian that accounts for the electronic energy in the atom, molecule, or solid (including kinetic energy, potential energy due to interactions with the nuclei, and electron-electron interactions), and $\mathscr{H}_{\mathrm{int}}(t)$ is an interaction Hamiltonian between the field-free system and the irradiated laser pulse. The HHG spectral response is found by solving the time-dependent Schrödinger equation defined by $\mathscr{H}$ and Fourier transforming the induced nonlinear polarization in the medium $\vec{p}(t) = \langle\Psi(t)|\vec{r}|\Psi(t)\rangle$, where $\Psi(t)$ is the time-dependent multielectron wave function. This problem typically does not have an analytic solution and is often very challenging to solve numerically. Still, considerable headway can be made by analyzing the symmetries of $\mathscr{H}$, which are generally spatiotemporal [dynamical symmetries (DSs)]. Whenever $\mathscr{H}$ is invariant under a unitary DS, the emitted HHG response follows strict restrictions in the form of selection rules. These may dictate the allowed harmonic orders (i.e., the HHG emission frequencies) and/or their polarization state [21].

HHG selection rules have been demonstrated and utilized for a number of applications, including shaping the high-harmonic polarization [22–26] and performing ultrafast spectroscopy for molecular symmetry [27], molecular orientation [28,29], chirality [30,31], and the carrier-envelop phase [32]. Here we propose an analogous symmetry-breaking spectroscopy approach for ring currents—we purposefully choose a probe laser pulse such that $\mathscr{H}$ is invariant under particular DSs that involve a reflection operation, imposing linearly polarized harmonics selection rules in ring-current-free media (i.e., the polarization of all allowed high harmonics is strictly linear along particular axes) [21]. However, if there is ring current in the medium then the reflection symmetry breaks, and harmonics are emitted with elliptical polarizations rather than linear, i.e., with polarization components transverse to the previously allowed emission. We shall show below that the intensity and ellipticity of the harmonic emission maps one-to-one the total ring current.

Notably, there is a major difference between DS breaking HHG spectroscopy of ring currents and of previously probed quantities that are based on symmetry breaking of $\mathscr{H}$ [27–30,32], as in this case $\mathscr{H}$ is always invariant under the symmetry in question. In other words, $|\Psi(t)\rangle$ itself leads to reflection symmetry breaking when it comprises an excited ring current, even though $\mathscr{H}$ is invariant under the reflection DS [because the sum of projections of $|\Psi(t)\rangle$ is not symmetric]. Utilizing this property, we can derive the explicit dependence of the harmonic response on the ring current. In the Supplemental Material (Sec. IV) [33], we analytically show that the HHG yield polarized transverse to the standardly allowed emission axis (i.e., the "forbidden" HHG emission) scales like the total ring current squared

$$I^{\perp}_{\mathrm{HHG}} \propto J^2_{\mathrm{ring}}, \tag{2}$$

where J_{ring} denotes the total ring current. More generally, we prove that the HHG ellipticity follows the relation

$$\varepsilon_{\mathrm{HHG}} \propto J_{\mathrm{ring}}/(B + J_{\mathrm{ring}}), \tag{3}$$

where B denotes a background emission from current-free states and is generally a function of the medium's ionization rate. For $J_{\mathrm{ring}} \ll 1$, $\varepsilon_{\mathrm{HHG}}$ depends linearly on J_{ring}, while for larger values the denominator can be Taylor expanded to yield a parabolic behavior. This analytical current-to-HHG mapping is highly convenient for a spectroscopic technique: the current can be exactly reconstructed from measurements.

Next, we explore several examples that demonstrate the applicability of the above analytical correspondence, starting with a pump-probe geometry schematically illustrated in Fig. 1(a): in step 1, a ring current is excited in the medium due to strong-field ionization from an intense circularly polarized pump laser pulse, which is subsequently probed in step (2) by an intense linearly polarized probe pulse. The probe pulse is polarized along the x axis and is therefore invariant under the reflection $y \to -y$ (denoted as σ_x). This standardly leads to x-polarized harmonic selection rules. Importantly, since the initial current excitation is circular, the pump pulse itself does not generate harmonics. Similarly, since the probe pulse is linear, it itself does not induce a ring current in the medium. Hence, the ellipticity of the high harmonics reflects the state of the initial current excitation, which is temporally resolved.

We numerically demonstrate this scheme using a noninteracting-electrons quantum model for neon, where the atom is occupied by four valence $2p_{m=\pm1}$ electrons (see Supplemental Material Secs. 1 and 2 [33]). Figures 1(b)–1(e) present the exemplary high-harmonic emission spectra and the average harmonic ellipticities vs the calculated ring current in the medium (which is varied by changing the duration of the pump pulse). When there is no current excitation (i.e., the pump's

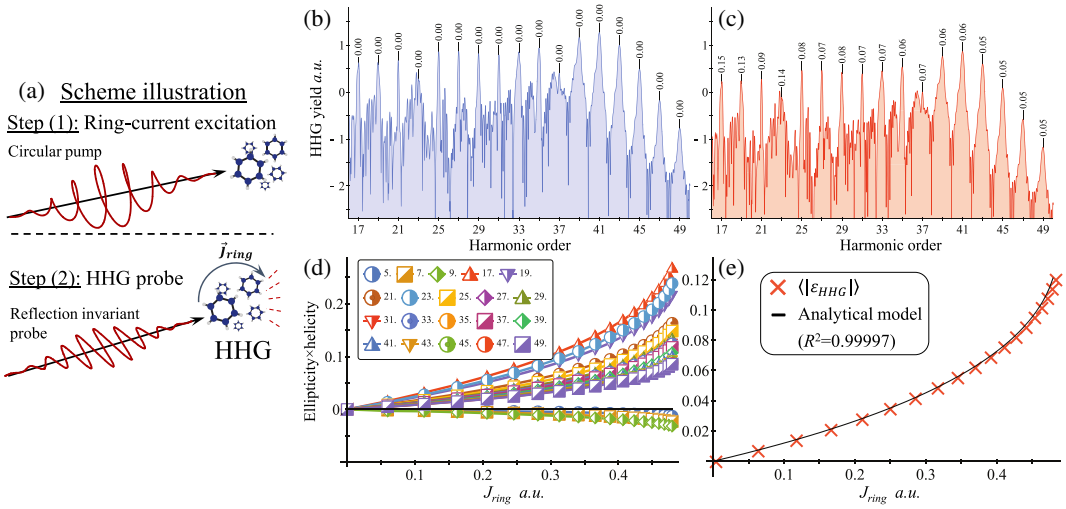

FIG. 1. (a) Pump-probe scheme illustration: a ring current is first excited in the medium by interaction with a circularly polarized pump. The medium is subsequently irradiated by an intense linearly polarized probe pulse that generates high-harmonic radiation, whose polarization state is correlated to the excited ring current. (b)–(e) Symmetry-breaking spectroscopy of ring currents in quantum model of neon using monochromatic pump and probe beams for $\lambda = 800$ nm. (b,c) HHG spectral yield with and w/o pump pulse, respectively. Harmonic ellipticities are indicated over each harmonic line showing that current-free media emit perfectly linear harmonics, while ring current-carrying media emit elliptical harmonics. (d) HHG emission ellipticity-helicity vs the ring current generated by the pump pulse (different lines indicate different harmonics). (e) Average HHG ellipticity vs ring current in the medium compared to analytical model given in Eq. (3). The plot calculated for pump power of 3.6×10^{14} W/cm^2, and probe power of 2×10^{14} W/cm^2.

duration is zero), the system is invariant under σ_x symmetry, so strictly linearly polarized harmonics are emitted [see Fig. 1(b)]. As stronger and stronger currents are excited, the HHG emission ellipticity increases, providing a background-free signal that corresponds to the ring current [see Fig. 1(c)]. Furthermore, the harmonics polarization helicity embeds the information on the ring current direction, since it changes sign if the ring current is reversed. Figure 1(d) shows that the ellipticity of all harmonics in the spectrum exhibits one-to-one mapping with J_{ring}. Figure 1(e) further plots the average ellipticity of harmonics in the spectrum vs J_{ring}, showing an extremely accurate fit to the formula in Eq. (3) ($R^2 = 0.99997$).

It is instructive to discuss the underlying mechanism responsible for the symmetry-breaking phenomenon. In the symmetric case (current-free media), each half-cycle of the probe pulse generates HHG emission that only differs by a π phase shift along the x axis. The emission from consecutive half-cycles interferes in time, leading to the generation of linearly polarized odd harmonics that uphold the symmetry-based selection rules. On the other hand, following the circular pump, a ring current is excited in the medium, because the $2p_{m=+1}$ states have a faster ionization rate than the $2p_{m=-1}$ states [16] (a ring current may also be excited by a circular pulse that is tuned to a transition [3,4]). This means that the electron density in the $2p$ shell carries angular momentum, which manifests in its interaction with the probe pulse by partially breaking the symmetry between consecutive half-cycles—the HHG emission between half-cycles now also differs by a π phase shift along the y axis (the y-polarized emission is nonzero because the bound state's angular momentum deflects the ionized electrons away from the x axis [13–16]). This effect lifts the reflection symmetry, while preserving the twofold discrete rotational symmetry that leads to odd-only harmonics [39]. As the current density increases, the ionized electrons are deflected further away from the x axis, causing stronger y-polarized emission in each half-cycle, therefore increasing the harmonic ellipticities. This mechanism is independent of the pulse envelope.

We next explore this scheme using a noninteracting-electrons quantum model for benzene molecules that captures the symmetry properties of benzene and its valence states (D_{6h} symmetry point group). In particular, we occupy four electrons in the equivalent of the π_2 and π_3 degenerate highest occupied molecular orbitals (see Supplemental Material [33] for details). Figures 2(a) and 2(b) present the HHG ellipticity vs the total ring current in randomly orientated benzene gas, showing similar results to those obtained in neon. Harmonic ellipticities form a background-free signal for ring current detection in benzene, closely following the behavior predicted by Eq. (3). In the Supplemental Material [33], we present almost identical results from aligned benzene when the alignment preserves the reflection symmetry of the probe (i.e., the C—C bond is aligned parallel or perpendicular to the x axis). Accordingly, from this point on we only consider aligned benzene gas where

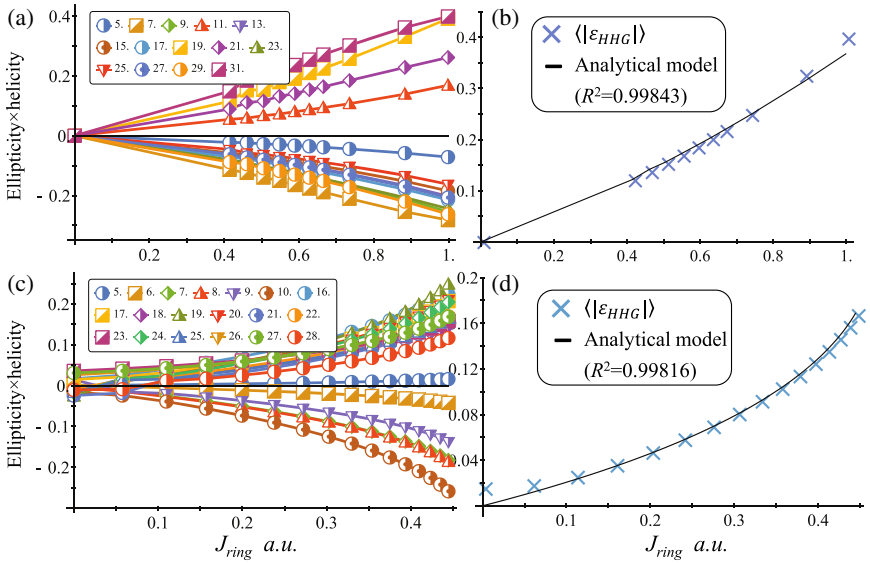

FIG. 2. Symmetry-breaking spectroscopy of ring currents in quantum models of benzene and neon systems. (a,b) Same as in Fig. 1(d), (e), but for orientation-averaged benzene medium, and with monochromatic linearly polarized probe pulses for $\lambda = 1700$ nm with probe power of 7×10^{12} W/cm^2 and pump pulses with power 1.1×10^{13} W/cm^2. (c)–(d) Same as in Fig. 1(d),(e), but using ω-2ω bi-chromatic cross-linear probe pulses, where even harmonics are also emitted with elliptical polarization due to the bi-chromatic scheme.

the C—C bond is parallel to the x axis, greatly reducing the computational time.

The above discussion focused on monochromatic ring current detection schemes, i.e., where both pump and probe beams have the same wavelength. This approach is favorable for experimental implementation, but leads to odd-only harmonic spectra. By adding a second harmonic (2ω) component to the probe beam, one can lift the twofold rotational symmetry in $\mathscr{H}$ that leads to odd-only harmonic generation. This effectively doubles the signal-to-noise ratio for the technique, since the number of measurable ellipticities is doubled. The addition of the 2ω component to the probe beam can be done in two different ways that preserve the reflection DS in $\mathscr{H}$: (i) the 2ω beam can be linearly polarized along the x axis, colinearly with the ω beam, or (ii) the 2ω beam can be linearly polarized along the y axis, cross linearly with the ω beam. In the colinear case, $\mathscr{H}$ upholds a "static" σ_x symmetry just as before. This approach leads to results similar to those in Figs. 1 and 2, except that even harmonics are also emitted (see Supplemental Material [33]).

We turn our attention to the cross-linear case. Here, $\mathscr{H}$ exhibits a reflection DS of the type $x \to -x$, $t \to +T/2$, where $T = 2\pi/\omega$ is the optical period. This DS imposes linearly polarized harmonics selection rules, where odd harmonics are x polarized and even harmonics are y polarized [21]. Unlike in the static symmetry case discussed above, the DS is only an approximate symmetry of $\mathscr{H}$, because the probe pulse has a finite temporal duration. Still, the selection rules are upheld as long as the probe pulse duration is much larger than T [40,41]. The advantage of using this scheme is that it typically leads to larger HHG ellipticities that are easier to detect. This is a result of the helical trajectory followed by the electron in each half-cycle when it is driven by the cross-linear probe pulse [40]—the emitted harmonic ellipticities are larger because the y-polarized emission in each half-cycle is larger to begin with. Figures 2(c)–2(d) present numerical results from the quantum model of neon with the ω-2ω cross-linear probe pulse, demonstrating that the sensitivity in the cross-linear scheme is larger (the average harmonic ellipticity is larger by roughly a factor of 2). Importantly, the analytical behavior derived in Eq. (3) is still upheld. Similar results are also obtained for benzene (see Supplemental Material [33]). We also note that slightly elliptical harmonics (up to ellipticity 0.04) are emitted from the current-free medium, because the probe pulse has a finite duration of ~22 fs.

So far, we have numerically investigated our technique with noninteracting electron models, which describes the qualitative behavior of ring currents and are effective for studying the mechanism behind HHG symmetry breaking. It is, however, also useful to perform quantitative *ab initio* calculations that include *e-e* interactions, because these allow exploring multielectron dynamics within the excited state. To this end, we have performed TDDFT calculations of HHG from excited ring currents in both neon and benzene using the OCTOPUS code [42–44] (see Supplemental Material [33] for details).

Figures 3(a)–3(c) present *ab initio* results from the monochromatic scheme in benzene that exhibits similar behavior to that observed in the noninteracting electron models. The main difference is that the average harmonic

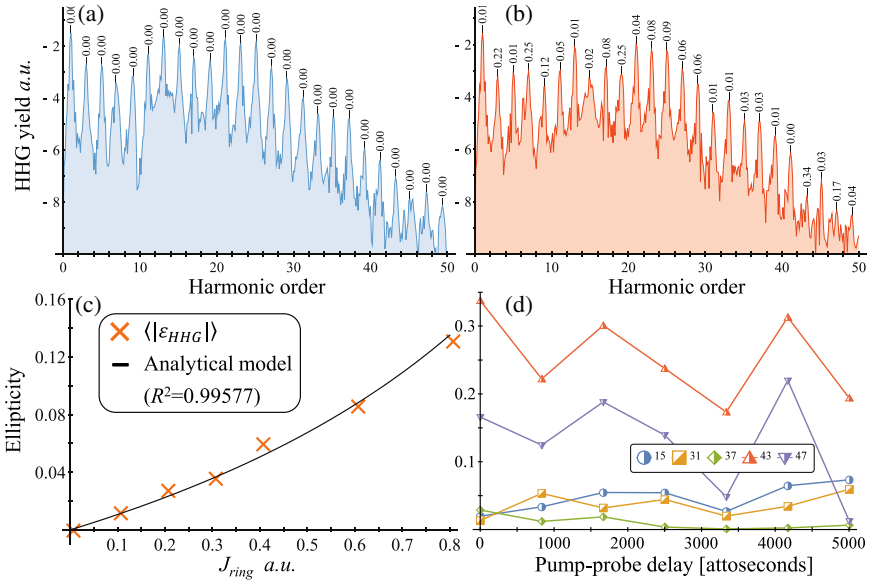

FIG. 3. Symmetry-breaking spectroscopy of ring currents in *Ab-initio* calculations in benzene using monochromatic pump and probe beams for $\lambda = 1250$ nm. (a,b) HHG spectrum with and w/o current excitation, respectively (harmonic ellipticities indicated in black over each harmonic order). (c) Average HHG ellipticity vs ring current in the medium compared to analytical model in Eq. (3). (d) Ellipticity of HHG emission vs the time-delay between current excitation and probe pulse for several selected harmonic orders, showing effects of *e-e* dynamics in the excited current which are imprinted onto the HHG emission. Plot calculated for probe power of 5×10^{13} W/cm^2.

ellipticity is slightly smaller in the *ab initio* calculation than in the quantum model (though still experimentally measurable [45]). This arises because the *ab initio* calculation also includes HHG emission from deeper states that do not carry angular momentum and are neglected in the quantum model (e.g., the $2s^2$ electrons in neon and sigma electrons in benzene). The Supplemental Material [33] presents similar *ab initio* results for neon.

Lastly, we explore the electron dynamics within the ring current by scanning the delay between the current excitation and the HHG probe pulse. It is important to point out that in the noninteracting electron models there is inherently no such dynamics, since in our case all bound states are exact eigenstates of $\mathscr{H}_0$ even after current excitation. Consequently, the harmonic ellipticities are delay independent in these models, reflecting the steady-state nature of ring currents. Thus, any delay-dependent harmonic ellipticities directly correspond to *e-e* interactions within the ring current.

Figure 3(d) presents the harmonic ellipticity vs the pump-probe delay for several selected highly oscillatory harmonics in benzene. Unlike in the noninteracting electron models, here the ellipticity of all the harmonics in the spectrum slightly oscillates on various timescales and amplitudes, though most harmonics vary weakly. Physically, this effect arises since the current-carrying multielectron wave function is not an exact eigenstate of $\mathscr{H}_0$. Thus, the electrons "breathe" (expand and contract) in response to the excitation by exerting classical coulomb forces on each other and quantum exchange and correlation. This dynamical process indicates the state of the ring current during its interaction with the probe pulse, which is imprinted on the harmonic emission. While the intensities of these oscillations may depend on the specific system and computational method, we verify that the effect is general, as it is observed in both neon and benzene systems using monochromatic and bichromatic probe pulses, as well as using different exchange-correlation functionals.

Notably, the largest variation in harmonic ellipticities is observed near "dips" in the HHG spectra [e.g., harmonics 15 and 31 in Fig. 3(b)]. These seem to be characteristic for multielectron effects in HHG and were previously observed in various forms [46–49]. We hypothesize that these photon energies are resonant to the characteristic timescale of the *e-e* interactions in the atom and molecule, making them highly susceptible to the electron dynamics in the current (because these energies correspond to particular electron trajectories [50] that sample the variation in the ring current between ionization and recombination times). Interestingly, different behavior is observed from neon (see Supplemental Material [33]), indicating the different nature of these multielectron systems. Most importantly, this phenomenon is experimentally accessible by our approach and may be used to explore the complex nature of many-body systems.

To summarize, in this Letter we have established HHG symmetry-breaking spectroscopy as a versatile, robust, and effective method for ring current characterization. We numerically explored the scheme in several geometries and in two model systems of neon and benzene. We showed

that it results in all-optical, ultrafast, background-free signals with one-to-one analytical correspondence between the ring current and the HHG emission. We further validated the scheme with *ab initio* calculations and predicted experimentally detectable *e-e* effects in the excited-current states.

We expect that this approach will prove highly useful for ultrafast molecular spectroscopy and for manipulating electronic currents in atoms, molecules, and solids. Importantly, the proposed technique is applicable for probing time-dependent ring currents by scanning the pump-probe delay (in which the temporal resolution is limited by the durations of the pump and probe pulses), as well as by analyzing the relative behavior of different harmonic orders. Furthermore, the spatial current density distribution in complex systems could potentially be probed by mapping the HHG emission to the initial transverse momentum of the ionized electrons. Extensions to oriented molecular media which are nonreflection symmetric are also possible. These exciting possibilities should be investigated in future work. Looking forward, a similar HHG symmetry-breaking approach can be implemented to characterize a variety of ultrafast phenomenon, e.g., topological, magnetic, electron correlation, etc., and we envision that it could advance the field of attosecond science.

This work was supported by the Israel Science Foundation (Grant No. 1781/18). O. N. gratefully acknowledges the support of the Adams Fellowship Program of the Israel Academy of Sciences and Humanities.

*ofern@tx.technion.ac.il
†oren@technion.ac.il

[1] T. C. Weinacht, J. Ahn, and P. H. Bucksbaum, Phys. Rev. Lett. **80**, 5508 (1998).
[2] H. Maeda, D. V. L. Norum, and T. F. Gallagher, Science **307**, 1757 (2005).
[3] I. Barth, J. Manz, Y. Shigeta, and K. Yagi, J. Am. Chem. Soc. **128**, 7043 (2006).
[4] I. Barth and J. Manz, Phys. Rev. A **75**, 012510 (2007).
[5] E. Goulielmakis, Z. H. Loh, A. Wirth, R. Santra, N. Rohringer, V. S. Yakovlev, S. Zherebtsov, T. Pfeifer, A. M. Azzeer, M. F. Kling, S. R. Leone, and F. Krausz, Nature (London) **466**, 739 (2010).
[6] S. Eckart, M. Kunitski, M. Richter, A. Hartung, J. Rist, F. Trinter, K. Fehre, N. Schlott, K. Henrichs, L. P. H. Schmidt, T. Jahnke, M. Schöffler, K. Liu, I. Barth, J. Kaushal, F. Morales, M. Ivanov, O. Smirnova, and R. Dörner, Nat. Phys. **14**, 701 (2018).
[7] Z. H. Loh, M. Khalil, R. E. Correa, R. Santra, C. Buth, and S. R. Leone, Phys. Rev. Lett. **98**, 143601 (2007).
[8] J. E. Moore, Nature (London) **464**, 194 (2010).
[9] M. C. Rechtsman, J. M. Zeuner, Y. Plotnik, Y. Lumer, D. Podolsky, F. Dreisow, S. Nolte, M. Segev, and A. Szameit, Nature (London) **496**, 196 (2013).
[10] K. J. Yuan and A. D. Bandrauk, Phys. Rev. A **92**, 063401 (2015).
[11] X. Zhang, X. Zhu, D. Wang, L. Li, X. Liu, Q. Liao, P. Lan, and P. Lu, Phys. Rev. A **99**, 013414 (2019).
[12] T. Heine, C. Corminboeuf, and G. Seifert, Chem. Rev. **105**, 3889 (2005).
[13] X. Xie, A. Scrinzi, M. Wickenhauser, A. Baltuška, I. Barth, and M. Kitzler, Phys. Rev. Lett. **101**, 033901 (2008).
[14] I. Barth and O. Smirnova, Phys. Rev. A **84**, 063415 (2011).
[15] T. Herath, L. Yan, S. K. Lee, and W. Li, Phys. Rev. Lett. **109**, 043004 (2012).
[16] I. Barth and M. Lein, J. Phys. B **47**, 204016 (2014).
[17] J. Kaushal, F. Morales, and O. Smirnova, Phys. Rev. A **92**, 063405 (2015).
[18] K.-J. Yuan, C.-C. Shu, D. Dong, and A. D. Bandrauk, J. Phys. Chem. Lett. **8**, 2229 (2017).
[19] K.-J. Yuan and A. D. Bandrauk, J. Phys. Chem. A **123**, 1328 (2019).
[20] P. M. Kraus, B. Mignolet, D. Baykusheva, A. Rupenyan, L. Horný, E. F. Penka, G. Grassi, O. I. Tolstikhin, J. Schneider, F. Jensen, L. B. Madsen, A. D. Bandrauk, F. Remacle, and H. J. Wörner, Science **350**, 790 (2015).
[21] O. Neufeld, D. Podolsky, and O. Cohen, Nat. Commun. **10**, 405 (2019).
[22] A. Fleischer, O. Kfir, T. Diskin, P. Sidorenko, and O. Cohen, Nat. Photonics **8**, 543 (2014).
[23] O. Kfir, P. Grychtol, E. Turgut, R. Knut, D. Zusin, D. Popmintchev, T. Popmintchev, H. Nembach, J. M. Shaw, A. Fleischer, H. Kapteyn, M. Murnane, and O. Cohen, Nat. Photonics **9**, 99 (2015).
[24] L. Medišauskas, J. Wragg, H. van der Hart, and M. Y. Ivanov, Phys. Rev. Lett. **115**, 153001 (2015).
[25] K. M. Dorney, J. L. Ellis, C. Hernández-Garc'ia, D. D. Hickstein, C. A. Mancuso, N. Brooks, T. Fan, G. Fan, D. Zusin, C. Gentry, P. Grychtol, H. C. Kapteyn, and M. M. Murnane, Phys. Rev. Lett. **119**, 063201 (2017).
[26] O. Neufeld and O. Cohen, Phys. Rev. Lett. **120**, 133206 (2018).
[27] D. Baykusheva, M. S. Ahsan, N. Lin, and H. J. Wörner, Phys. Rev. Lett. **116**, 123001 (2016).
[28] E. Frumker, N. Kajumba, J. B. Bertrand, H. J. Wörner, C. T. Hebeisen, P. Hockett, M. Spanner, S. Patchkovskii, G. G. Paulus, D. M. Villeneuve, A. Naumov, and P. B. Corkum, Phys. Rev. Lett. **109**, 233904 (2012).
[29] P. M. Kraus, A. Rupenyan, and H. J. Wörner, Phys. Rev. Lett. **109**, 233903 (2012).
[30] O. Neufeld, D. Ayuso, P. Decleva, M. Y. Ivanov, O. Smirnova, and O. Cohen, Phys. Rev. X **9**, 031002 (2019).
[31] D. Ayuso, O. Neufeld, A. F. Ordonez, P. Decleva, G. Lerner, O. Cohen, M. Ivanov, and O. Smirnova, arXiv: 1809.01632v2 [Nat. Photonics (to be published)].
[32] O. Neufeld, A. Fleischer, and O. Cohen, Mol. Phys. **117**, 1956 (2019).
[33] See Supplemental Material at http://link.aps.org/supplemental/10.1103/PhysRevLett.123.103202 for details about the methodology used in numerical calculations presented in the main text, as well as some complementary results, including the analytical derivation of the mapping between the harmonic emission response and the ring current, which includes Refs. [34–38].
[34] F. Ceccherini and D. Bauer, Phys. Rev. A **64**, 033423 (2001).

[35] J. A. Fleck, J. R. Morris, and M. D. Feit, Appl. Phys. **10**, 129 (1976).
[36] M. D. Feit, J. A. Fleck, and A. Steiger, J. Comput. Phys. **47**, 412 (1982).
[37] J. P. Perdew and A. Zunger, Phys. Rev. B **23**, 5048 (1981).
[38] C. Hartwigsen, S. Goedecker, and J. Hutter, Phys. Rev. B **58**, 3641 (1998).
[39] N. Ben-Tal, N. Moiseyev, and A. Beswick, J. Phys. B **26**, 3017 (1993).
[40] M. Kitzler, X. Xie, A. Scrinzi, and A. Baltuska, Phys. Rev. A **76**, 011801(R) (2007).
[41] D. Shafir, Y. Mairesse, D. M. Villeneuve, P. B. Corkum, and N. Dudovich, Nat. Phys. **5**, 412 (2009).
[42] M. A. L. Marques, A. Castro, G. F. Bertsch, and A. Rubio, Comput. Phys. Commun. **151**, 60 (2003).
[43] A. Castro, H. Appel, M. Oliveira, C. A. Rozzi, X. Andrade, F. Lorenzen, M. A. L. Marques, E. K. U. Gross, and A. Rubio, Phys. Status Solidi B **243**, 2465 (2006).
[44] X. Andrade, D. Strubbe, U. De Giovannini, A. H. Larsen, M. J. T. Oliveira, J. Alberdi-Rodriguez, A. Varas, I. Theophilou, N. Helbig, M. J. Verstraete, L. Stella, F. Nogueira, A. Aspuru-Guzik, A. Castro, M. A. L. Marques, and A. Rubio, Phys. Chem. Chem. Phys. **17**, 31371 (2015).
[45] L. Barreau, K. Veyrinas, V. Gruson, S. J. Weber, T. Auguste, J.-F. Hergott, F. Lepetit, B. Carré, J.-C. Houver, D. Dowek, and P. Salières, Nat. Commun. **9**, 4727 (2018).
[46] H. J. Wörner, H. Niikura, J. B. Bertrand, P. B. Corkum, and D. M. Villeneuve, Phys. Rev. Lett. **102**, 103901 (2009).
[47] J. P. Farrell, B. K. McFarland, M. Gühr, and P. H. Bucksbaum, Chem. Phys. **366**, 15 (2009).
[48] A. Rupenyan, P. M. Kraus, J. Schneider, and H. J. Wörner, Phys. Rev. A **87**, 031401(R) (2013).
[49] D. A. Telnov, K. E. Sosnova, E. Rozenbaum, and Shih-I. Chu, Phys. Rev. A **87**, 053406 (2013).
[50] P. B. Corkum, Phys. Rev. Lett. **71**, 1994 (1993).